International Journal of Innovative
Computing, Information and Control
Volume **18**, Number **4**, August **2022**

ICIC International ©2022 ISSN 1349-4198
pp. 1181–1201

A RUBBER TREE ORCHARD MAPPING METHOD VIA IMAGE PROCESSING

Worawut Kunghun and Akapot Tantrapiwat

Department of Mechanical Engineering
Faculty of Engineering
King Mongkut's Institute of Technology Ladkrabang
1, Chalongkrung Road, Ladkrabang, Bangkok 10520, Thailand
{ 59601321; akapot.ta }@kmitl.ac.th

Received November 2021; revised March 2022

Abstract. *This research was carried out in order to evaluate the performance of a computer visual mapping method using permanent targets mounted on the tree trucks as the distinctive marks to the environment. Two targets per tree trunk were used to create sufficient target perception from a distance. The computer vision uses the known distance between these two targets to determine the location of the camera using pin-hole camera principle. The system was designed based on configurations of the rubber tree orchard which is one of the main industrial crops in South East Asia. A set of experiment was carried out on both laboratory and real plantation site. With different parameters and setup, the mapping system was able to achieve the RMS maximum error 43.06 mm in laboratory control environment and 114.57 mm in actual site. This magnitude of error was considered acceptable in low accuracy autonomous operation in automatic agricultural tasks such as watering, fertilization and harvest. Several aspects regarding parameters in the mapping method setup and the outcome were discussed and compared.*
Keywords: Mapping, Navigation, Rubber tree orchard, Image processing

1. **Introduction.** Rubber tree is a perennial plant that can live for over two years, making it a perfect cash crop. This particular plant plays a major role in generating income and has a huge impact on the lifestyles of the population of rural areas in Thailand, specifically in the southern part of the country. Moreover, since 1991, Thailand has been the largest rubber producer in the world, and it plays a significant role as the main exporter of rubber [1,2]. The demand for rubber has increased, which has affected the price; based on movements in the rubber prices at the Hat Yai Central Rubber Market, located in the southern part of Thailand, the average price of ribbed smoked sheets-3 (RSS3) in 2021 was 45-70 THB/kg. Over the past few decades, the price has increased steadily, which led, in February 2009, to the highest average price for RSS3: 146 THB/kg. The RSS3 price, from 2002-2011, grew by around 15 percent per year. In fact, rubber prices depend considerably on the global market and futures markets such as the Tokyo Commodity Exchange (TOCOM), the Singapore Commodity Exchange (SICOM), and the Future Exchange of Thailand (AFET) [3]. Therefore, the Thai government does not have the power to control or influence rubber prices. Even though Thailand is the largest rubber producer in the world, it still has little or no bargaining power due to variations in rubber prices and uncertainties about the income level of farmers and labor cost trends. In addition, Thailand's rubber industries are struggling due to low profits and high labor costs. Moving on to the process of production, harvesting latex sap is tedious work that requires large amounts of manpower, and the rubber trees must be maintained. To

DOI: 10.24507/ijicic.18.04.1181

minimize these workloads and the costs associated with production, automation for the rubber tree orchards will be increasingly involved in the agricultural system. The most important part of designing an autonomic vehicle that can be used in rubber tree orchards is designing a navigation system to allow the vehicle to move around. This is considered one of the most important factors due to the complicated topography of the plantations that the vehicle needs to traverse. Moreover, it is also challenging to design a low-cost system that is affordable for farmers. Therefore, choosing the right navigation technology is critical; this research will now describe the various navigation system technologies that have been adopted to solve this problem.

In recent years, sensors, global positioning systems (GPSs), LiDAR, laser scanners, and ultrasonic geometrical measurements have been employed in automatic vehicles for agricultural systems. These technologies have been improved to further study the autonomous navigation of robots in rough topography. Autonomous navigation and orchard mapping have been studied and tested for many applications. Bayar et al. developed a novel model-based control strategy for a self-driving agricultural vehicle that works in fruit tree orchards. The method relies on data from a planar laser scanner, as well as wheel and steering encoders, for location estimation and path following, unlike other methods that use data from GPS signals [4]. In a simulated tree plantation nursery, Khot et al. developed a sensor fusion technique for determining the navigational posture of a skid-steered mobile robot. The robot's location and orientation were determined using real-time kinematic GPS (RTK-GPS) and dynamic measurement unit (DMU) sensors [5]. Keicher and Seufert also designed an agricultural vehicle guidance system. Several sensors, including mechanical, global navigation satellite system (GNSS), machine vision, laser triangulation, ultrasonic, and geomagnetic sensors, were used to generate position, attitude, and direction-of-movement information for control algorithms [6]. For simpler terrain configurations and using fewer sensors, Barawid Jr. et al. created an automatic guidance system capable of guiding an autonomous vehicle between tree rows in real time. They used a laser scanner as a navigation sensor and concentrated primarily on the straight-line detection of tree rows [7]. Liu et al. developed a tightly coupled integrated navigation system for unmanned ground vehicles (UGVs) that integrates two-dimensional (2D) LiDAR, an inertial navigation system (INS), and odometry. An efficient LiDAR-based line-feature detection/tracking technique is developed to assess the relative changes in the orientation and displacement of the vehicle [8]. Li et al. reviewed guidance technology research for agricultural autonomous vehicles and mapping; GPS, machine vision, dead-reckoning sensors, laser-based sensors, inertial sensors, and geomagnetic direction sensors are some examples of the most commonly used techniques. To extract features and important data, they applied computational approaches to sensor information. The locations of the sensors and their accuracy were used to control the actuators in the steering and driving system for navigation [9]. Other approaches have used modern camera and image processing methods to perform mapping or to determine the location of a vehicle in an orchard. Shalal et al. showed that a machine vision system can be used as an alternative to navigation. However, the working environment or surroundings, including variations in the precise locations of the objectives, have an impact on this system. Furthermore, camera calibration, image analysis, and the feature extraction of navigation parameters are used to compensate for factors such as the lack of bright, and constant light sources. All of these factors make the implementation of autonomous vehicles in the agricultural setting more complex. When it is time for autonomous vehicles to get to work, they can easily move between tree rows. One of the most extensively used techniques for locating trees in a row is the data fusion of vision systems and laser scanners or LiDAR [10-12]. Benet and Lenain demonstrated that autonomous vehicles could recognize natural items

blocking or surrounding them, such as tree trunks, grass, and leaves. When navigation is performed using the fusion of sensor and camera data, detection is critical for safety reasons. When the vehicles encounter barriers, they must either cross or avoid them, with the exception of a large solid object; in this case, the vehicles must stop [13]. For a specific type of plantation, Xue et al. developed a novel, variable-field-of-view machine vision method that enables agricultural robots to travel between rows in cornfields. The method uses an image processing algorithm to recognize directed lines and engaging morphological characteristics in far, near, and lateral fields of view. Fuzzy logic control is used by the mobile robot to allow it to maneuver along the guided lines [14]. For rubber tree plantations, Zhang et al. developed a rubber-tapping robot with autonomous navigation and a gyroscope to collect information on a rubber forest. The sparse point cloud data of tree trunks are extracted using low-cost LiDAR and a gyroscope using the clustering method. The autonomous automobile traverses a given lateral distance along one row, stopping at fixed points, turning from one row to another, and gathering data on plant spacing, row spacing, and tree diameters [15]. Pirat et al. developed a method using a single monocular camera to distinguish LED signals from reflected sunlight. The innovative and simple formulation of the measurement equations allows the unambiguous identification of rotations from data translation between the target and chaser docking ports. The performance of lateral control by docking two CubeSats has an accuracy of less than 1 cm [16]. The method of using a camera with a fabricated vision environment therefore seems to be an alternative that allows one to obtain better accuracy without the use of multiple sensors. The method was tested in our previous, preliminary study in order to determine the parameters and configuration of a rubber tree plantation using the pin-hole camera method [17,18]. Although methods using high-performance sensors along with a digital camera are effective, other approaches using modern AI technology can be used to enhance the image processing of the images from the camera, and they make it unnecessary to use expensive sensors. Kim et al. created path detection for autonomous orchard travel. A patch-based convolutional neural network (CNN) is used in the proposed approach for image classification to achieve path area segmentation, which involves cropping image patches from an input image with a sliding window and generating a path score map with a four-layer CNN for tree and path classification, path area segmentation, and target path detection with boundary line determination [19]. Shin et al. developed practical preprocessing strategies for effective deep neural network training. A deep convolutional neural network extracts and detects the features of a region in an image for road crack detection and then classifies the image based on the features [20]. Fujiyoshi et al. demonstrated how deep learning is applied to each picture identification task, as well as describing deep learning-based autonomous driving and the associated problems [21]. Blok et al. validated the applicability of two probabilistic localization algorithms for in-row robot navigation in orchards using a 2D LiDAR scanner. This study focused on an orchard robot's in-row navigation and did not discuss autonomous turning or obstacle and headland detection [22]. While previously mentioned works either involve the use of advanced sensors or complicated image processing with artificial intelligence (AI) technology, which requires large datasets, other approaches utilize additional objects in the environment, such as targets or marks that are set up in the work field. These methods are effective when they are applied to certain types of environments, such as rubber tree orchards in which the trees are fully grown and the pattern of the plantation is suitable. Targets that are mounted on tree trunks can be easily maintained and made distinct from the surrounding environment. This simplifies image processing across a wide variety of landscapes and allows mapping to be done by using the trees directly.

In this research, the rubber tree orchard and plantation were studied. Their configurations were used to establish proper materials and methods for the computer visual mapping system. The mapping method using two permanent targets mounted on each tree trunk and the pin-hole camera principle was analyzed and implemented. This led to the establishment of orchard geometry and coordinate system in relation to the target positioning obtained from computer vision which used a series of image processing techniques to extract the targets from the environment. The geometry parameters were then examined and assigned their optimum values in experimentation which were done in both laboratory controlled environment and the actual plantation sites. The performance of the mapping system determined by average errors was measured and compared with different parameter setup.

2. Materials and Methods.

2.1. **Rubber tree plantation.** Rubber research and development are controlled by the Rubber Authority of Thailand, which advises local rubber farmers. As shown in Figure 1, rubber tree orchards have unique configurations, with trees typically planted in a row and column pattern. On certain terrains, such as steep hills or along a flat terrain, this pattern can be varied, but this is rare. The planting density is around 80 trees per Rai, which is the typical Thai farming area unit; it is equivalent to 1,600 m^2. Each farmer has a different system of working in the orchard. Normally, farmers walk between the rows until they end, and then they walk between the columns for systematic collection. The ground vehicle path was designed to fit perfectly with each rubber tree orchard's unique characteristics, as shown in Figure 1(a). Sap is harvested from rubber trees by workers walking along the columns. Each column requires regular maintenance to simplify the daily collection process. The autonomous or mapping system must imitate this pattern. The plantation surveys were conducted on actual rubber plantation in Phrae Province, Northern Thailand. The orchard terrains are often flat, although some of the rubber farms may be grown in small inclined areas such as a foothill. Along the tree row, each tree is usually planted 3 m away from another. The diameters of the tree trunks varied from 120 to 200 mm. On a plantation site, many uncontrollable parameters such as the trunk straightness, rough planting sites, and the inconsistency of the light can affect

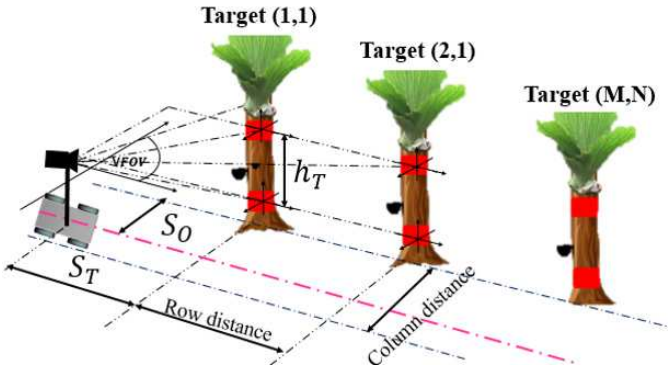

(a) Model orchard for autonomous mapping

(b) Installation of separate red targets on each rubber tree trunk

FIGURE 1. Rubber tree orchard

the navigation system. The straightness of the rubber tree trunk was an uncontrollable parameter affecting the calculations, where the mean stem inclination in randomized trials was approximately 3-10 degrees. These parameters were examined and compared when the system was tested in the laboratory in a controlled environment [17]. The orchard used in this research had conditions similar to those found in most rubber tree plantations in Thailand and Southeast Asia. The sap collecting container, shown in Figure 1(b), is placed higher than the ground level to hold the sap from the rubber tapping process. Traditionally, these containers are made of ceramic material, but plastic is now used as well. These containers can be used as one of the targets on the tree trunk if their colour and size are suitable. However, in this research, the targets were made by strapping two bands made out of sheet metal and painted red around the trunk, as shown in Figure 1(b). Both target straps were 100 mm wide and wound around the trunk's circumference. Other factors need to be considered when choosing the target material and the placement of the targets. These targets remain unprotected on the tree trunks for a long time; they may become dirty and covered by moss or weed. It is very important to keep the targets clean so that they can be detected by the camera, as shown in Figure 1(b). The size of the target is related to the ability of the camera to detect the target from a distance. Placing one large target on the tree trunk was not feasible, and two separate targets were used instead. There were two target distances used in this study, 500 and 700 mm. These two distances were obtained from the initial study. In that work, it was found that too small a distance between the two targets will result in less precision when the targets are further away from the camera. On the other hand, a distance that is too large causes parts of the targets to be out of frame when the camera is placed close to the targets. In the preliminary study, three target distances, 300, 500, and 700 mm, were studied. It was found that 300 mm was not a practical target distance due to the space limitations of the tree trunk; there must be enough space to allow the sap to be harvested. Moreover, a target distance of 700 mm will allow a camera with a vertical field of view (VFOV) of 43.30 degrees and a resolution of 720 × 1280 pixels to detect both targets in the image frame when the camera is about 1 m away from the tree trunk.

2.2. **Camera visual localization using pinhole model technique.** To compute the position of the tree trunk using the camera, the common pinhole model was developed and used [17,18]. Figure 2 shows a diagram of the pinhole model comprising the target planes projected through the camera lens onto the sensors of the image plane. Modern digital cameras use Charge Coupled Device (CCD) sensors that can also be applied to other

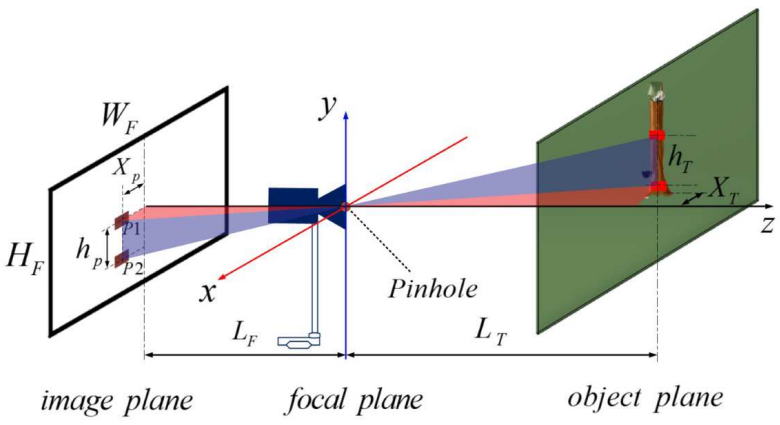

FIGURE 2. Pinhole camera model for target position estimation

types of images, such as X-ray images, scanned photographs from enlarged negatives, and scanned photographic negatives. The pinhole model of Figure 2 shows the relationship between the object plane and image plane according to the position of the tree trunk relative to the camera. The object plane has a parameter that is necessary for creating an orchard geometry model. The offset length between the camera and the tree row on the world coordinate system is based on farmers' movement through the tree rows. The separate red targets installed on each tree trunk specify each rubber tree trunk's position in the orchard. The red targets were recorded by a webcam, as shown in Figure 3(a), and they appear on the image plane shown in Figure 3(b). When a target of a known size is captured, the position of the image frame can be determined from the proportions of the

(a) Two separate targets on each rubber tree in an uncontrolled environment of an actual tree orchard

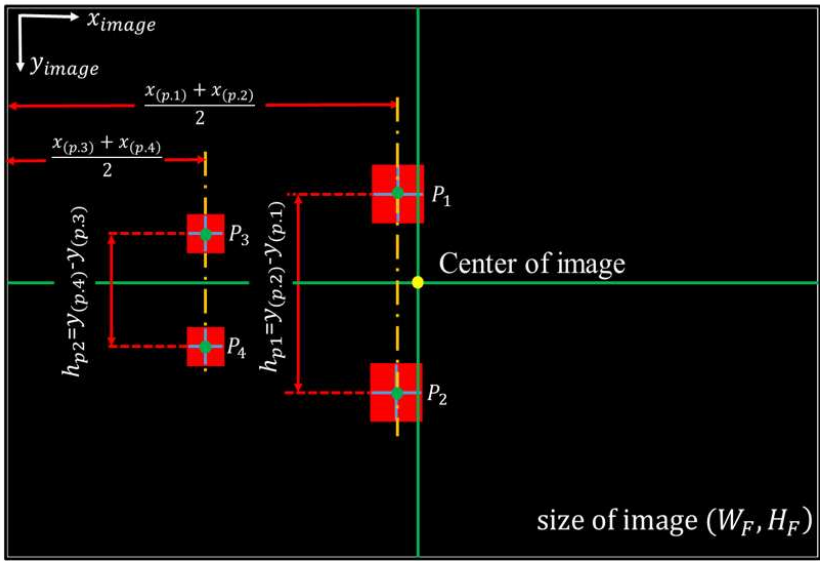

(b) Position of binary image frame (x, y) coordinate systems

FIGURE 3. Two separate red targets fixed on each rubber tree and projected on the image frame

image position and size according to the ratio of the triangles from both actual objects and image frames. The image position and size were measured in terms of the number of pixels. The vertical axis was used as the y-axis, and it was parallel to the tree trunk. The width of the image frame was used as the x-axis, which represented the distance between the tree trunk and another tree. The z-axis was placed perpendicular to the image frame. The distance between the image frame and the camera focal point, as well as the distance between the focal point and the tree trunk, lay on the z-axis. When a target of a known size is captured, the length L_T from the target to the pinhole, usually located in front of the camera lens, can be determined by

$$L_T = L_F \frac{h_T}{h_p} \tag{1}$$

The length between the lens and the sensor plane of the camera is written as L_F. The known height of the target lying vertically on the world coordinate is written as h_T, while h_p, as the height of the target in the image frame, is determined by the number of pixels in the y-direction of the image frame. Because a similar triangle was also applied for the x-axis, the distance between the reference point and the target can be determined in the same manner. In this geometry, the reference point was set at the center of the camera projection. Equation (2) was used for distance estimation in the x-direction:

$$X_T = X_p \frac{h_T}{h_p} \tag{2}$$

where X_T is the offset length between the camera and the tree row in the world coordinate system and X_p is the pixel length between the center of the image and the position of the target shown in the image frame in the horizontal direction. Equations (1) and (2) indicate that both X_T and L_T significantly depend on other factors, such as the camera configuration and the proportions of the image from the camera frame. Better distance estimation can be achieved by increasing the target size. The latex tapping process is performed on the tree trunk. If only one target is placed on each tree trunk, the relative distance of this target from the camera cannot be compared and converted to actual distances in the world coordinate system. When the camera moves further away from the object, the object's size becomes smaller, and when the camera approaches the object, the image becomes larger. It is necessary to have two targets to measure the pixel length between them using the image coordinate system. Thus, two separate targets were required; they resemble one large target at a distance. The orchard images, as shown in Figure 3(a), were captured and processed via a series of image processing techniques, and the positions of the two separate red targets on the image plane were then located. These two extracted red patches were then used to determine the actual tree position using Equations (1) and (2). Figure 3(b) shows the primary targets P1 and P2 on the image plane near the camera, and the secondary targets P3 and P4 are further from the camera. The camera follows the pathway of the rubber tree in Figure 3(a) and selects the nearest rubber tree trunk as its primary target. h_{p1}, as the pixel length in the y-direction, is found from the image frame and used to calculate the target-camera distance (S_T) and the positions P1, P2 and P3, P4 in the x-direction; the average is needed because the tree trunk is not perfectly straight. The secondary targets used to identify the camera's orientation were obtained from Equation (6). The positioning data, as shown in Figure 3(b) on the image frame, must be converted into an orchard geometry model for vertical vision navigation to determine the camera direction. After the orchard image was captured, all red target images were extracted and converted to binary images, as described previously. It is important to establish the relationships between

the red patches in the images. Targets at greater distances produce smaller red patches, while each tree provides a pair of targets. The binary image displays the number of red patches in the frame, as shown in Figure 3(b). The mid-point between the red patches was recognized as the position of the rubber tree in the vertical image plane. In Figure 3(b), the horizontal positions, in pixels, of the targets in the image planes $x_{(p.1)}$, $x_{(p.2)}$, $x_{(p.3)}$ and $x_{(p.4)}$ are the pixel coordinates in the x-direction, while $y_{(p.1)}$, $y_{(p.2)}$, $y_{(p.3)}$ and $y_{(p.4)}$ are the vertical pixel positions in the y-direction. The height of a pixel h_{p1} can be calculated using the pixel positions $y_{(p.1)}$ and $y_{(p.2)}$, which correspond to the far tree trunk, while the height h_{p2} can be calculated using the pixel positions $y_{(p.3)}$ and $y_{(p.4)}$, which correspond to the nearer tree trunk. h_{p1}, as the pixel length in the y-direction, is shown in an image frame. The two separate red targets appear on the image nearest to the center of the image frame as P1 and P2 for the further targeted trees, as shown in Figure 3(b). The upcoming targeted tree trunk will then move closer to the center of the image frame. The conversion of positions P1 and P2, using information acquired by the pinhole model to determine the camera's position in the plantation site, can also be performed using the relationship between the horizontal vision navigation and the object plane. Figure 4 illustrates the horizontal model in the world coordinate system; this is also one of the vital angles for tracking the two separate red targets fixed on the rubber tree trunk. These two red targets were constructed of 0.35-mm-thick metal material to prevent damage from the humid environment, as shown in Figure 3(a). The red target plates had a width of 100 mm and were installed around the rubber tree trunk. To navigate the camera through the orchard, new coordinate parameters were established that are related to the tree row and column geometry. As stated earlier, rubber collection is usually conducted along the tree rows. Therefore, the navigation and mapping processes were created using the same configuration. Figure 4 shows the target-camera distance parallel to the tree row (S_T) and the offset distance between the camera and the tree row (S_O) as independent parameters that can be calculated by inputting the target and orchard fixed parameters together with the camera orientation in relation to the tree row (θ). The camera pinhole method can locate the target regardless of the orchard geometry. When the primary and secondary targets, known by their positions in a given row of the orchard, were captured and their positions in the image frame were determined, the target-camera distance, S_T, was obtained from Equation (3):

$$S_T = \frac{\left\{h_T \cdot \left[L_F \cdot \cos(\theta) + \left|\left(\frac{x_{(p.1)}}{2} + \frac{x_{(p.2)}}{2} - \frac{W_F}{2}\right)\right| \cdot \sin(\theta)\right]\right\}}{\left(y_{(p.2)} - y_{(p.1)}\right)} \tag{3}$$

In the same manner, the offset distance, S_O, was calculated using the following equations:

$$S_O = \frac{\sqrt{2} \cdot h_T \cdot \sqrt{{L_F}^2 + {P_i}^2 - {L_F}^2 \cdot \cos(2\theta) + {P_i}^2 \cdot \cos(2\theta) - 2 \cdot L_F \cdot |P_i| \cdot \sin(2\theta)}}{2 \cdot \left(y_{(p.2)} - y_{(p.1)}\right)} \tag{4}$$

and

$$P_i = \left(\frac{x_{(p.1)}}{2} + \frac{x_{(p.2)}}{2} - \frac{W_F}{2}\right) \tag{5}$$

The camera orientation relative to the tree row, θ, is a fixed parameter in Figure 4 and should be assigned a proper value. If this angle is too small, the camera will point along the tree row and the targets will enter the image frame from a far distance. In other words, the targets will enter the image frame too soon. This will result in difficulty evaluating the size of the targets because they are too small. By contrast, if θ is too large, the camera will point in the direction of the tree column or perpendicular to the tree row. The target will enter the image frame too slowly. In other words, the camera has

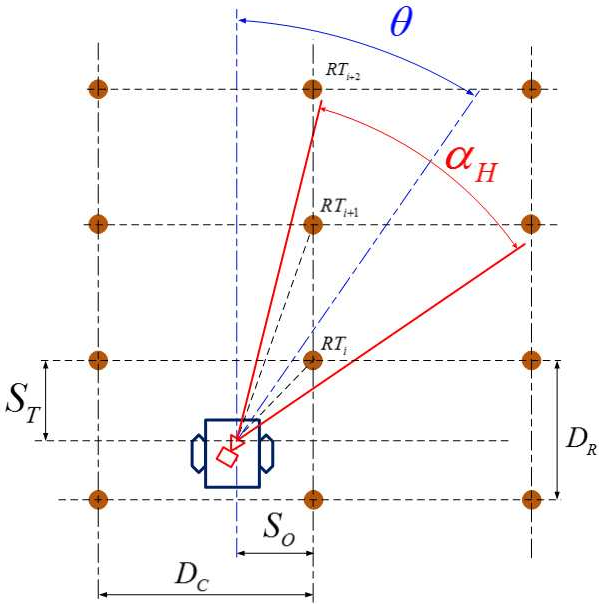

FIGURE 4. Horizontal vision mapping object plane of the orchard geometry model

to move closer to the target before it can enter the image frame. This configuration will decrease the ability of the method to determine the camera's distance from the targets. When navigating the camera along the tree row, it is impossible to maintain the camera orientation at all times. Alternate angles of the camera will affect the target detection, as previously described. It is more convenient to establish a dependent parameter that can identify the orientation of the camera relative to the initial fixed angle. The relative orientation θ_C can be used as the navigating orientation, and it is determined based on the orchard and target fixed parameters together with the fixed orientation, θ, as shown by Equation (6). The target perception ability and orchard mapping ability are greatly dependent on θ. In reverse, the optimal θ should be chosen depending on the camera's field of view in the horizontal direction, the orchard row and column distances, and the target height in the vertical direction.

$$\theta_C = \theta - \sin^{-1}\left(\frac{h_T \cdot \left(\frac{1}{\left(y_{(p.4)} - y_{(p.3)}\right)} \cdot (P_{i-1}) - \frac{1}{\left(y_{(p.2)} - y_{(p.1)}\right)} \cdot (P_i)\right)}{D_R}\right) \tag{6}$$

when

$$P_i = \left(\frac{x_{(p.1)}}{2} + \frac{x_{(p.2)}}{2} - \frac{W_F}{2}\right) \tag{7}$$

$$P_{i-1} = \left(\frac{x_{(p.3)}}{2} + \frac{x_{(p.4)}}{2} - \frac{W_F}{2}\right) \tag{8}$$

As mentioned earlier, the distance between the two targets on the tree trunk plays an important role in the determination of the target distance. The distances between the two targets were studied and compared. The configuration of the vertical layout between the targets and the camera is shown in Figure 5. In this configuration, the camera is placed in the middle plane, and both the targets on the tree trunk are horizontally symmetric to the middle plane. The ideal configuration provides a relationship between the vertical image size in pixels and the two red targets installed on the rubber tree. The camera

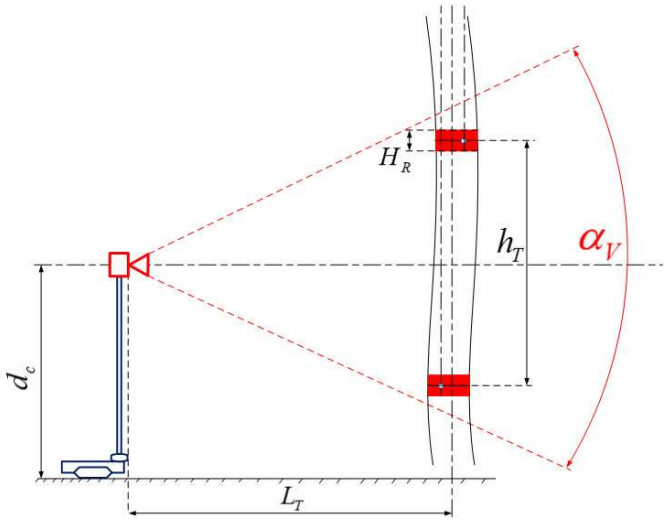

FIGURE 5. Vertical vision mapping object plane of the orchard geometry model

used to obtain such images must be able to cover the upper and lower vertical red targets mounted on the rubber tree. Each camera model has limitations in terms of its vertical field of view (VFOV). The length parameter L_T represents the distance of the target to the pinhole and the height of the target in the world coordinate system is written as h_T. This is a variable that must be calculated to ensure that the two red targets will both appear in the image; it can be estimated using Equation (9):

$$\alpha_V = 2\tan^{-1}\left(\frac{\frac{(h_T+H_R)}{2}}{L_F \cdot \frac{h_T}{h_p}}\right) \tag{9}$$

2.3. **Image processing.** The location of rubber trees for field mapping is considered the physical appearance of the rubber tree. The color of the trunk of the rubber tree is very similar to the color of the surrounding environment. As previously described, the targets were mounted on the tree trunks. The image areas of these targets, classified as the region of interest (ROI), had a different color than the surrounding environment. The red target has a different color than the environment, as shown by the hexadecimal RGB code of this color. The red-green-blue components are $(255, 0, 0)$. The red target represents the only major color difference visible in the environment, although the environment of the rubber plantation changes with the seasons. The detected red targets were also used to calculate the image frame's height parameter for object distance estimation in the orchard geometry model using Equations (3) and (4). Images of the separate red targets were recorded by a webcam, a Logitech C 920 camera. This camera can record real-time video at a resolution of 720 × 1280 pixels with a frame rate of 30 FPS, a horizontal field of view (HFOV) of 70.42 degrees, and a vertical field of view (VFOV) of 43.30 degrees. Figure 6(a) shows the two separate red targets on the tree trunk in the form of an RGB image, which is an image with a color system composed of the three primary colors: red, green, and blue. The red target is installed on a tree trunk in a real-world environment, and the red-green-blue component values do not conform to color theory. The actual red-green-blue component values in the actual environment are the following: red 170-255, green 50-100, and blue 50-200. This is because lighting conditions throughout the orchard are not equal. The images received directly from the webcam required enhancement to better identify the targets. A series of image processing techniques were used to sharpen the images. These methods include the unsharp masking system (USM). As shown in Figure 6(a), each

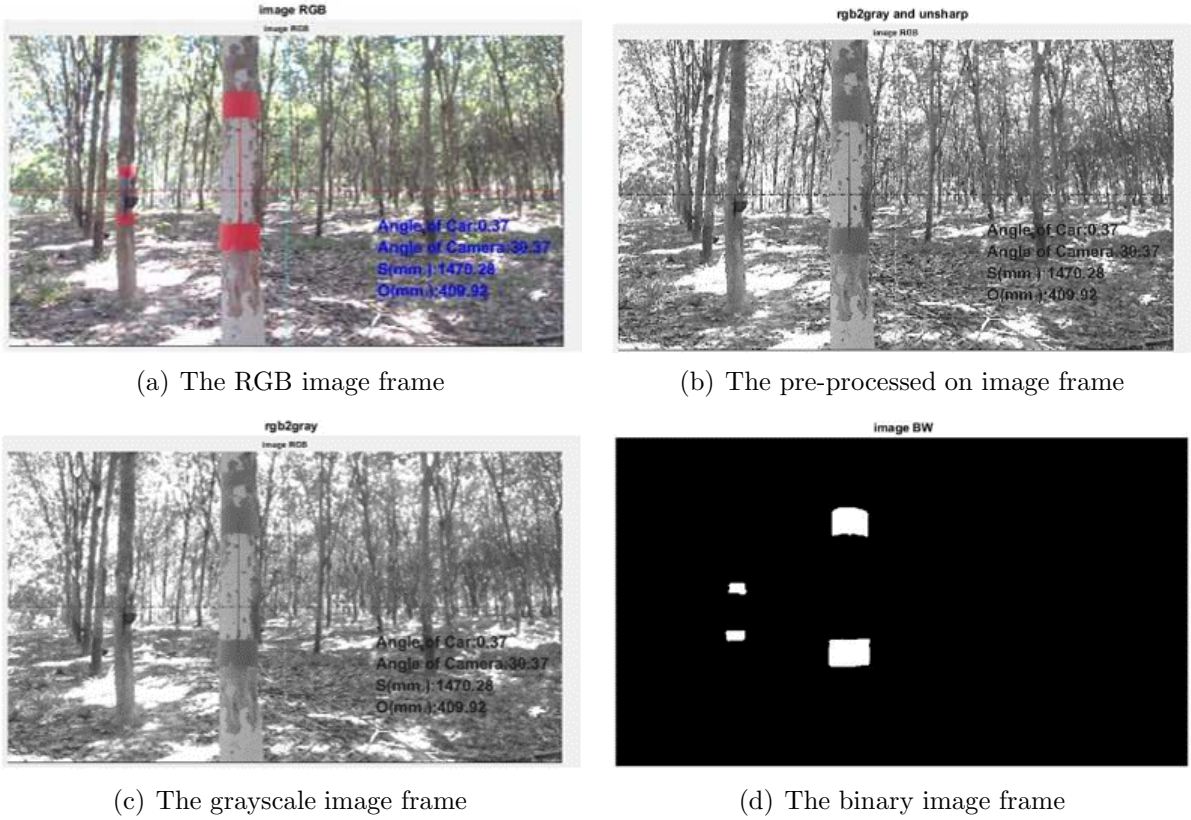

(a) The RGB image frame

(b) The pre-processed on image frame

(c) The grayscale image frame

(d) The binary image frame

FIGURE 6. Image processing process detects the separated red targets

frame of the received real-time webcam video has a different brightness level, so we need to increase the sharpness of the images. At a frame rate of 30 FPS, we use the snap image processing technique. There are changes in both the laboratory and orchard environments at all times. As a result, each image has a different brightness level at the beginning of the image processing pipeline. Figure 6(b) shows an image that has been sharpened by increasing the contrast at the edges of each pixel using the USM technique with a Gaussian low-pass filter with a standard deviation of 1. This argument controls the size of the region around the edge pixels that is affected by the sharpening. A large value sharpens wider regions around the edges, whereas a small value sharpens narrower regions around the edges. The image was also converted into grayscale, as shown in Figure 6(c), with a color intensity from 0-255 (8 bit). The image frame converts RGB values to grayscale values by performing a weighted sum of the R, G, and B components. The coefficients used in calculation of grayscale values are identical to the luminance calculation which is a part of ITU-R BT.601-7 in the recommendation of International Telecommunication Union Radio communication Sector (ITU-R). These values were determined and rounded into three decimal places. After each pixel in the entire image (720 $\times$ 1280 pixels) has been converted to grayscale, Rec.ITU-R BT.601-7 calculates a weighted sum: R has a weight of 0.299, G has a weight of 0.587, and B has a weight of 0.114. After the areas of the two red targets were determined, the grayscale images were converted into a binary form containing two intensities, 0 and 1. Any pixel with the value of 0 was displayed in black, while any pixel with a value of 1 was shown in white. The binary image defines a referenced gray intensity value known as the threshold value. As shown in Figure 6(d), this value was obtained by averaging at 90-115 possible different shades of gray from black to white for this specific application. The gray concentration was adjusted over

time depending on the lighting conditions, especially in the red target area. The rubber tree is detected using the image processing and conversion process described previously; the rubber tree appears in the image frame at various positions depending on the actual location of the rubber tree relative to the camera's position. The size of the target on the rubber tree that can be detected depends on the distance from the target to the camera. In fact, the image processing pipeline in use can detect many targets in the real rubber plantation area. However, the two targets, or trees, that are closest to the camera will be used to map the camera's position. The sizes of the largest targets in the two frames are determined and compared to all binary images of the area so that the target as close to the camera as possible can be selected from the total number of targets. Mapping the locations of trees in the rubber plantation allows us to locate the camera because the rubber plantation is laid out in a row pattern, and the camera moves along the rows of rubber trees in order to be able to see the targets. Therefore, it is necessary to mount the camera so that it faces toward a given rubber tree, which will result in the camera being at an angle relative to the row line of the rubber tree, as shown in Figure 4. Figure 6(d) depicts a binary image of a rubber tree. The first set of targets near the center of the image represents a rubber tree near the camera. The second set of targets, further away from the center of the picture, represents a rubber tree that is further away from the camera. The target detection method only works for a maximum distance of 6 m from the target rubber tree, so the camera can see two target trees and calculate the distance between them. This image processing system determines the center of the white positions shown in the binary image, as depicted in Figure 6(d). The two white positions near the center of the image frame represent the tree trunk near the camera, and the two white positions that are further away represent the tree trunk that is further from the camera. The positions P1, P2, P3, and P4 in Figure 3(b) are also shown in Figure 6(d); these positions were previously used to calculate the pixel length (h_p) for the equation representing the orchard geometry model.

3. **Experimentation.** It is important to test the mapping system's performance and accuracy; the parameters S_O and S_T in the image processing algorithm are important for navigating real rubber plantations. Experiments were performed to compare the results from the laboratory and the results from a real rubber tree orchard. First, experiments were performed in the laboratory with controllable parameters, such as upright rubber tree trunks, a constant amount of light, and flat surface areas. Second, experiments were performed in an uncontrollable environment, a real rubber tree orchard. The difference is that the parameters in the actual rubber tree orchard cannot be controlled in the same way that parameters used in the laboratory can be controlled. The area in the natural rubber plantation to be used as the experimental area was randomly selected. In the laboratory, the rubber tree trunk mockup and areas for testing were designed to be similar to the rubber tree orchard. The laboratory had a replica of a rubber tree; the trunk was made of plastic, as shown in Figure 7(a). The trunk had a diameter of 125 mm, and the red targets were installed on the replica tree, as shown in Figure 7(b). The red targets were made of 0.5-mm-thick sheet metal and installed by wrapping them around the mockup tree. The height and width of the red target are 100 and 125 mm, respectively. Furthermore, the two red targets were installed at distances of 500 and 700 mm, respectively. The installed red targets should be consistent with the height of the rubber tree, and the heights considered should be consistent with the height of the actual rubber tapping area on a real rubber tree. The experiment involves moving the camera along the rows of simulated rubber trees. This lab experiment creates a virtual test area to determine how the cameras should move along the line of trees. The test site is built based on the actual

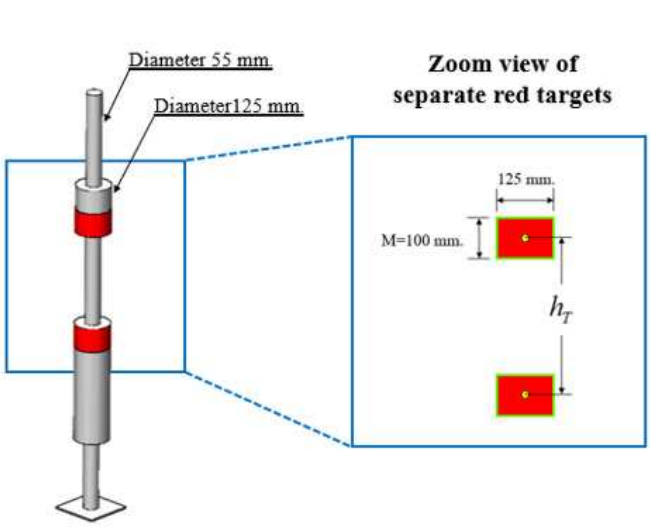

(a) Rubber tree trunk mockup

(b) Tree trunk mockup testing area in the laboratory

FIGURE 7. Testing area using world coordinate in the laboratory

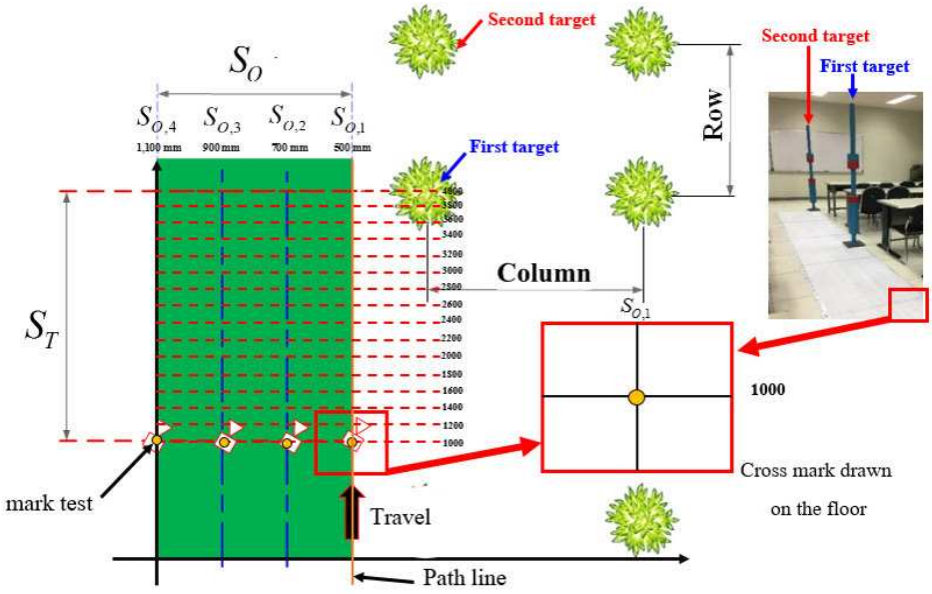

FIGURE 8. Experimental layout used during laboratory testing

distance between sets of coordinates on a flat area; a marking pen was used to draw a tile grid on the floor. Figure 7(b) shows the setup used to measure the actual distance to the ground to know how far the camera moves from the target rubber tree. The coordinate system used is similar to that of the rubber tree orchard in the previous section (Figure 8). Inside the 4 × 1.1 m test area, 64 positions representing grid intersections with intervals of 0.2 m were designated. The vehicle velocity system will be designed in the future with a speed of approximately 0.2-0.3 m/s, which is a reasonable movement speed for a vehicle working in a rubber plantation. In the experimental setup depicted in Figure 8, the tracking performance of the image processing method along the path line was evaluated by changing the separation of the red targets to 0.5 and 0.7 m. In the course of the laboratory experiments, 64 position values were obtained by approximation using

(a) Computer vision mapping during the experiment

(b) Example installation of metal plates on rubber tree trunks

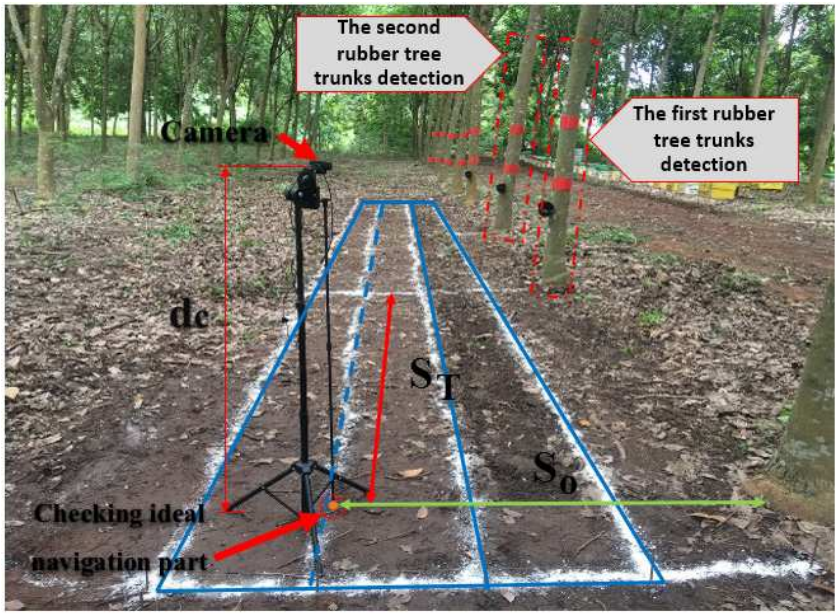

(c) Testing area on the world coordinate in the orchard

FIGURE 9. Orchard experimental setup in the orchard

an image processing algorithm. Such experiments are evaluated to determine the error of the mapping method. The proposed marking system had a satisfactory performance in the laboratory, and it was then tested at a rubber tree orchard, as shown in Figure 9(a). The coordinate system setup was similar to that described in the previous section. Inside the 4×1.1 m test area, 64 positions representing grid intersections, with intervals of 0.2 m, were designated. Each rubber tree was equipped with two red metal plates, as shown in Figure 9(b). The two separate red targets did not interfere with rubber tapping collection. As shown in Figure 9(c), the camera was set up to receive images for processing. The camera was installed at the center of the two separate red targets. In a real rubber plantation, the ground is rough, with uneven platform conditions in the test area. Preparation of the test area was performed by using a small string to create real distances in real-world coordinates. The method used to measure the distances was the same as that used in the laboratory experiments, as shown in Figure 8. A plantation in

(a) Rubber tree trunks for actual testing (b) Trunk mockup for testing in the laboratory

FIGURE 10. Red targets installed on each rubber tree trunk for testing

Northern Thailand (18°07'00.0"N, 100°09'00.0"E) was selected as the testing site. The experiments took place between 7:00 and 11:00 am to be consistent with harvesting and to allow the rubber planters to carry out various tasks. The experiments shown in Figure 10 are meant to measure the accuracy of the navigating system, which involves using image processing and the orchard geometry to guide autonomous vehicles in rubber tree plantations. The trials are not dependent upon the use of sensor technology for navigation. This study carried out a comparison between a laboratory experiment and an experiment in a real rubber field. The experiment will focus on navigability and controllable and uncontrollable external factors, such as stable and unstable quantities, flat and uneven ground conditions, and the straightness of the rubber trees. Therefore, the effects of these factors must be tested so that the errors caused by the tested parameters will be known in the future. The variables S_O and S_T were the variables that we needed to test by comparing laboratory experiments with experiments at real rubber plantation sites; these experiments will measure the error of the developed system. From Equations (1) and (2), there are two variables, X_p and h_p, that are directly obtained from the mapping process, and the following environmental effects must be considered: lighting conditions, the resolution of the camera, and the flatness of the ground. These must be woven together to ensure that such a system can still perform mapping, which in turn can be used for the navigation of the system in the future. The goal of this system is to reduce costs for farmers and perform actual navigation.

4. **Results and Discussion.** From Equations (3) and (4), the variables S_O and S_T are used for mapping; these equations are generated from the orchard geometry model. Comparing them allows us to analyze the real factors that caused the obtained errors. The results, as shown in Figure 11 and Figure 12, track the performance of the image processing algorithm in mapping a rubber tree orchard. This is a comparison of the system's performance in the laboratory and on the plantation. It can be clearly seen that the magnitude of the error of the image processing algorithm system was different throughout the testing area. We propose using error space indicators from area navigation in the rubber tree orchard to estimate the error space of navigating using the image processing system. We define an error space indicator to evaluate the quality of the area grid and the position error. The parameters used to measure S_O and S_T were tested using the value of the magnitude of the space error. The error space is shown in Figure 11 and Figure 12. These figures show the trend of error values in the test area, and they include data from 46 error points in an area of 4.4 m^2. The magnitudes of the error values are displayed in 3-D graphs with S_O, S_T, and mapping error axes.

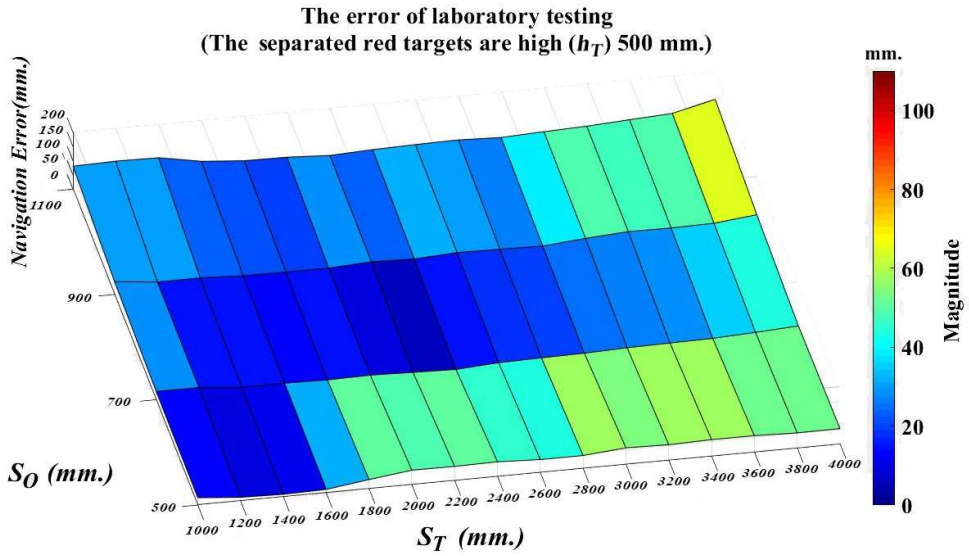

(a) The two separate red targets (h_T) by 500 mm

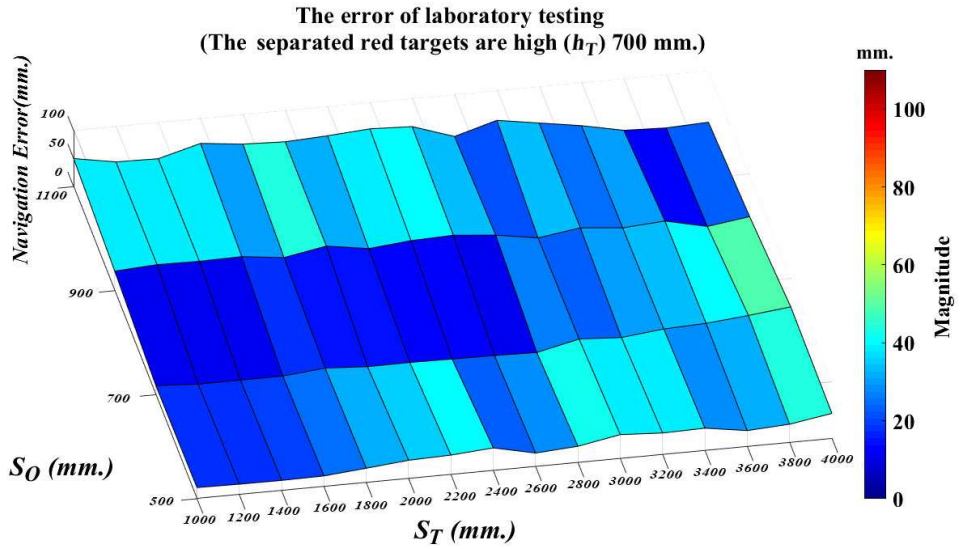

(b) The two separate red targets (h_T) by 700 mm

FIGURE 11. (color online) The magnitude of error in area testing for controlled environment (laboratory testing)

Figure 11 shows the magnitude of error in area testing for a controlled environment (laboratory testing). The heights of the targets are 500 mm and 700 mm, respectively. The error space is smooth, indicating a constant error. However, the magnitude of the error varies across the 46 measured positions in the test area. When the target height is 700 mm, the error values are smaller than when the target height is 500 mm, as shown in Figures 11(a) and 11(b), respectively. The experiment shows that in a controlled environment (laboratory testing), the method performs in a satisfactory manner. This experiment was compared with an experiment in a real rubber tree orchard to show how different factors affect the mapping system. Figure 12 shows the error space for an uncontrolled environment (orchard testing). The error values at the 46 locations differ in size from those of the laboratory experiment, as shown in Figures 12(a) and 12(b). The error values for the rubber tree orchard are different at each measurement point. In an uncontrolled

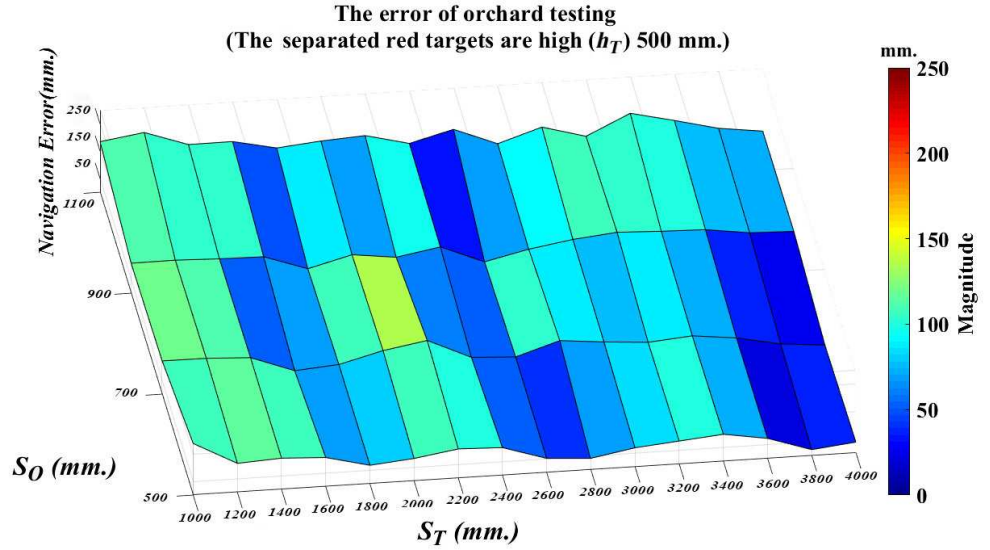

(a) The two separate red targets (h_T) by 500 mm

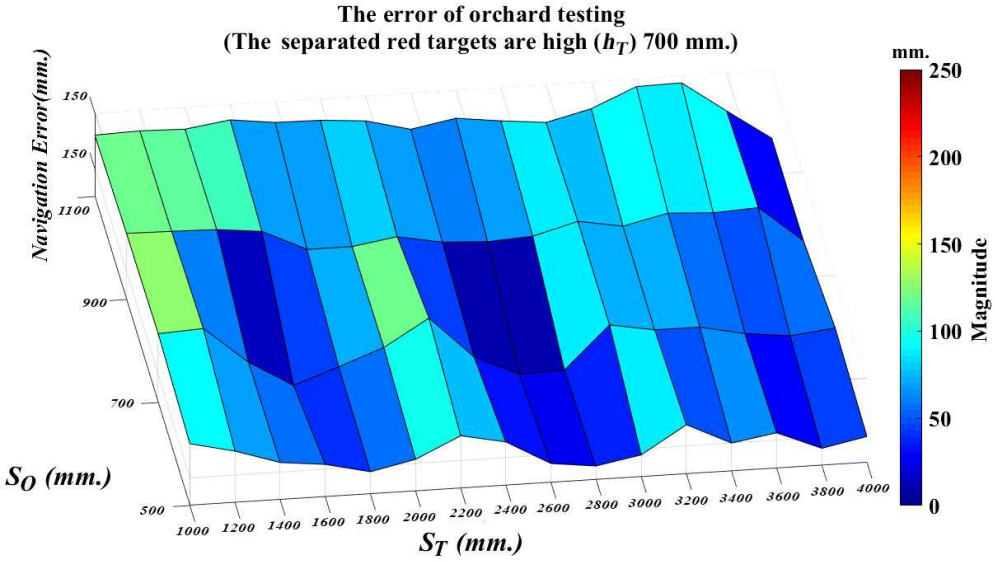

(b) The two separate red targets (h_T) by 700 mm

FIGURE 12. (color online) The magnitude of error in area testing for controlled environment (orchard testing)

environment, the main factor that increases the error is the unstable lighting conditions at different times. The results are consistent with laboratory experiments: the average error is greater when the height of the target is 500 mm and it is smaller when the height of the target is 700 mm. The error space for navigation using the image processing system shows that the presented strategy allows one to obtain accurate solutions in an efficient way. The reason behind this is related to the rubber tree plantation site, since it has different lighting conditions when compared to the controlled environment. The real rubber tree shown in Figure 10(a) is not perfectly straight, while the mockup in the laboratory shown in Figure 10(b) is perfectly straight. The performance of the navigating system was tested by using two different length between the separated red targets: 500 and 700 mm. The parameters used to demonstrate the efficiency of the method are the maximum error and the root mean square error, which represents the mean squared error in the experimental area. The

performance of the mapping system shown in Figure 13 indicates that when the camera was far from the test target, more errors occurred compared to when the camera was near the target. In a controlled environment such as the laboratory, the navigation error was much smaller than in an uncontrolled environment. The camera moved along one row and the root mean square error (RMS) of the mapping performance was calculated using controlled environment tests. The length between the two targets at different separation lengths of 500 and 700 mm were measured RMS difference from 43.06 mm and 32.42 mm, respectively, showing that the method had excellent path tracking performance. The RMS was used to compare the two targets with different separated lengths 500 mm is 1.33 times more than 700 mm. The maximum error was coherent with the root mean square error, while the two different separate lengths gave maximum errors of 100.26 mm and 55.55 mm, respectively. As shown in Figure 14, for the orchard testing case, the RMS was calculated for the two different target separation lengths of 500 and 700 mm, and was obtained at 114.57 mm and 99.82 mm respectively. It can be seen that the error from smaller target distance, 500 mm, results in 115% greater than the average error obtained from target distance at 700 mm. When considering the maximum errors throughout the test area, as shown in Figure 12, the 500 mm target distance produced error at 258.62 mm, while the 700 mm target distance gave 198.82 mm of the maximum error. In a controlled environment, the errors had smaller variation throughout the test plane, while in an uncontrolled environment, the fluctuation seems to increase significantly, but the error values were considered acceptable. From the experimental results shown in Figure 13 and Figure 14, we predicted the trend of the navigation error as a 2D image. This will allow us to compensate for future errors as the autonomous vehicle moves through the rubber tree orchard.

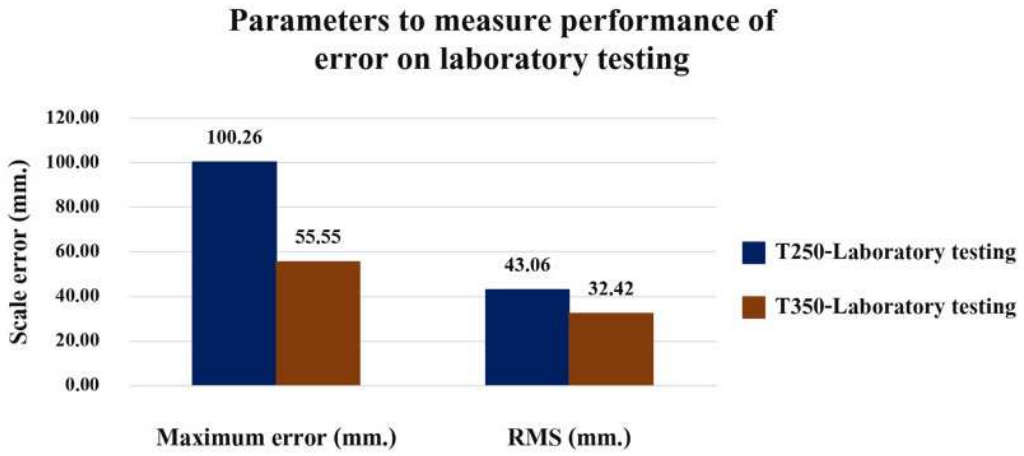

FIGURE 13. Mapping performance results in laboratory testing

5. **Conclusion.** Previous researches used the following technologies to find objects in an orchard environment: sensor technology, such as laser scanners and LiDAR sensors, GPS, image processing, and artificial intelligence (AI). Then, the location of the object was converted periodically for navigation. The most accurate approach is to use a sensor technology system, but the cost is relatively high, approximately 90-13,000 USD. These prices are referenced by the brand SICK's Sensor Solutions, which is a leader in sensor intelligence and application solutions, and they are widely used in this industry. The price depends on the accuracy of the system, the ability of the system to search for objects, and other technical capabilities that are necessary for a navigation system for an autonomous

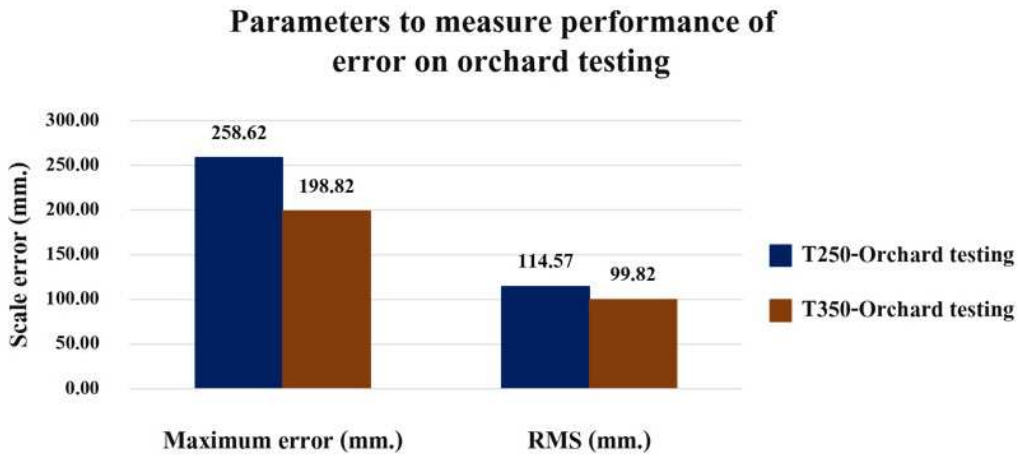

FIGURE 14. Mapping performance results in orchard testing

agricultural vehicle. This would result in the cost being high for autonomous systems. Image processing technology has been applied to a variety of engineering solutions. Compared to sensor technology, image processing can be used to develop a very cheap navigation system. An image processing system is less accurate than sensor technology. However, image processing technology has another disadvantage. It needs to be tested in an environment that can be used to adjust the threshold variable. Previous studies have presented an error rate of no more than 15 cm in the image processing pipeline [14]. To extract the ROI from the image processing system, image conversion techniques are used. The location of the object of interest is then displayed. Computers are now cheaper and more efficient, which is why AI technology is used to find objects in images [19,21]. AI technology provides a number of advantages, including the elimination of the requirement for a processing procedure; however, the disadvantage is that we have to use large number of images to properly train the model to perform in a given environment. We propose the method described in this research because, when compared to previous methods, it has the following advantages: the cost of using it for automation in the orchard is cheap, and it uses less processing hardware and software. When compared to sensor technology, this method does have a larger error value. Although this error seems to be large, the mapping method is still feasible. Because an autonomous system for agriculture can be designed for low-speed tasks, the vast area of an orchard can also provide marginal space to compensate for this magnitude of errors.

The orchard mapping method from this research has effectively estimated position of the camera in relation to the target distance (S_T) along the tree row and the offset distance (S_O) to the tree row. These two measured distances can be used to navigate through the orchard by a suitable autonomous system. In the actual plantation site, the errors were double in comparison to the laboratory experiment. It was caused by the uncontrollable environment, such as flat terrain, consistent target position, bright and constant light sources, and the errors from the parameters that were converted to cooperate with the geometrical position in the rubber tree orchard. The magnitudes of errors in the S_T-direction and S_O-direction were large, but effective navigation of the autonomous vehicle in the rubber tree orchard was still feasible. Future studies can design autonomous vehicles using a navigating system that accounts for hills and uneven ground to study the effect of movement velocity on real-time position accuracy. The navigating system needs to compensate for terrain uncertainty. The rubber tree orchard algorithm was shown to

be consistent with the actual rubber tree orchard environment and showed promise for reliable mobile robot localization and navigation in the future.

REFERENCES

[1] Rubber Authority of Thailand, Rubber Research Institution of Thailand, *Thai Rubber Statistics*, http://www.rubber.co.th, Accessed on October 8, 2021.

[2] C. Musikavong and S. H. Gheewala, Ecological footprint assessment towards eco-efficient oil palm and rubber plantations in Thailand, *Journal of Cleaner Production*, vol.140, no.2, pp.581-589, 2017.

[3] A. Romyen, P. Sausue and S. Charenjiratragul, Investigation of rubber-based intercropping system in Southern Thailand, *Kasetsart Journal of Social Sciences*, vol.39, no.1, pp.135-142, 2018.

[4] G. Bayar, M. Bergerman, A. B. Koku and E. I. Konukseven, Localization and control of an autonomous orchard vehicle, *Computers and Electronics in Agriculture*, vol.115, pp.118-128, 2015.

[5] L. R. Khot, L. Tang, S. Blackmore and M. Nørremark, Navigational context recognition for an autonomous robot in a simulated tree plantation, *Bioresource and Agricultural Engineering*, vol.49, no.5, pp.1579-1588, 2006.

[6] R. Keicher and H. Seufert, Automatic guidance for agricultural vehicles in Europe, *Computers and Electronics in Agriculture*, vol.25, nos.1-2, pp.169-194, 2000.

[7] O. C. Barawid Jr., A. Mizushima, K. Ishii and N. Noguchi, Development of an autonomous navigation system using a two-dimensional laser scanner in an orchard application, *Biosystems Engineering*, vol.96, no.2, pp.139-149, 2006.

[8] S. Liu, M. M. Atia, T. B. Karamat and A. Noureldin, A LiDAR-aided indoor navigation system for UGVs, *The Journal of Navigation*, vol.68, no.2, pp.253-273, 2015.

[9] M. Li, K. Imou, K. Wakabayashi and S. Yokoyama, Review of research on agricultural vehicle autonomous guidance, *International Journal of Agricultural and Biological Engineering*, vol.2, no.3, pp.1-16, 2009.

[10] N. Shalal, T. Low, C. McCarthy and N. Hancock, A preliminary evaluation of vision and laser sensing for tree trunk detection and orchard mapping, *Proc. of Australasian Conference on Robotics and Automation*, University of New South Wales, Sydney Australia, 2013.

[11] N. Shalal, T. Low, C. McCarthy and N. Hancock, Orchard mapping and mobile robot localisation using on-board camera and laser scanner data fusion – Part A: Tree detection, *Computers and Electronics in Agriculture*, vol.119, pp.254-266, 2015.

[12] N. Shalal, T. Low, C. McCarthy and N. Hancock, Orchard mapping and mobile robot localisation using on-board camera and laser scanner data fusion – Part B: Mapping and localisation, *Computers and Electronics in Agriculture*, vol.119, pp.267-278, 2015.

[13] B. Benet and R. Lenain, Multi-sensor fusion method for crop row tracking and traversability operations, *Proc. of AXEMA-EURAGENG Conference*, Paris, France, 2017.

[14] J. Xue, L. Zhang and T. E. Grift, Variable field-of-view machine vision based row guidance of an agricultural robot, *Computers and Electronics in Agriculture*, vol.84, pp.85-91, 2012.

[15] C. Zhang, L. Yong, Y. Chen, S. Zhang, L. Ge, S. Wang and W. Li, A rubber-tapping robot forest navigation, *Sensors Journal*, vol.19, 2019.

[16] C. Pirat, F. Ankersen, R. Walker and V. Gassa, Vision based navigation for autonomous cooperative docking of CubeSats, *Acta Astronautica*, vol.146, pp.418-434, 2018.

[17] W. Kunghun and A. Tantrapiwat, Development of a vision based mapping in rubber tree orchard, *Proc. of the 4th International Conference on Engineering, Applied Sciences and Technology (ICEAST2018)*, Phuket, Thailand, pp.206-209, 2018.

[18] W. Kunghun, A. Tantrapiwat and P. Chaidilokpattanakul, Navigation of autonomous vehicle for rubber tree orchard, *Proc. of the 5th International Conference on Engineering, Applied Sciences and Technology (ICEAST2019)*, Luang Prabang, Lao PDR, pp.252-255, 2019.

[19] W.-S. Kim, D.-H. Lee, Y.-J. Kim, T. Kim, R.-Y. Hwang and H.-J. Lee, Path detection for autonomous traveling in orchards using patch-based CNN, *Computers and Electronics in Agriculture*, vol.175, 2020.

[20] Y. Shin, M. Kim, K.-W. Pak and D. Kim, Practical methods of image data preprocessing for enhancing the performance of deep learning based road crack detection, *ICIC Express Letters, Part B: Applications*, vol.11, no.4, pp.373-379, 2020.

[21] H. Fujiyoshi, T. Hirakawa and T. Yamashita, Deep learning-based image recognition for autonomous driving, *IATSS Research*, vol.43, no.4, pp.244-252, 2019.

[22] P. M. Blok, K. van Boheemen, F. K. van Evert, J. IJsselmuiden and G.-H. Kim, Robot navigation in orchards with localization based on Particle filter and Kalman filter, *Computers and Electronics in Agriculture*, vol.157, pp.261-269, 2019.
[23] R. Hartley and A. Zisserman, *Multiple View Geometry in Computer Vision*, 2nd Edition, Cambridge University, 2003.
[24] E. Trucco and A. Verri, *Introductory Techniques for 3-D Computer Vision*, 2nd Edition, Prentice Hall, 1998.

Author Biography

Worawut Kunghun, currently a Lecturer at the Robotics and Automation Engineering Department, Panyapiwat Institute of Management, is now pursuing his Ph.D. degree at the Department of Mechanical Engineering, School of Engineering, King Mongkut's Institute of Technology Ladkrabang. He has more than 10 year experience in teaching and research in mechanical engineering relating mechanical design and automatic control systems.

Akapot Tantrapiwat received his Ph.D. in 2009 from Lehigh University, Pennsylvania, USA. He is currently working as a full time assistant professor at the Department of Mechanical Engineering, School of Engineering, King Mongkut's Institute of Technology Ladkrabang. His field of interests includes mechanical design, manufacturing and automation, AI technology in mechanical applications.